Paper III

Dagestad, K-F. and Olseth, J.A. (2005)

An alternative algorithm for calculating the cloud index

Manuscript

An alternative algorithm for calculating the cloud index

Knut-Frode Dagestad and Jan Asle Olseth
Geophysical institute
University of Bergen
Allegaten 70
5009 Bergen
Norway

April 2005

Abstract

The cloud index is an important component of the Heliosat algorithm, which estimates solar radiation components from Meteosat High Resolution Visible images. The cloud index quantifies the reflective properties of the atmosphere, and varies from 0 at clear conditions to 1 at overcast. The algorithm is semi-empirical in the way that it includes several constants that need to be tuned. Some of these were removed in the Heliosat-II algorithm (Rigollier et al., 2004) which introduced the Meteosat calibration constant to replace the "pseudo reflectivity" with a "real reflectivity". This approach is followed here, and two additional changes are made: 1) An analytical expression is introduced to correct for backscattered radiation from air molecules. 2) A correction is made for non-lambertian reflectivity, removing the time consuming need for determining the ground reflectivity for each month and each slot. The new cloud index is used to calculate global irradiances which are validated against hourly measurements from five European ground stations. The average root mean square deviation is 15.5% for a six month spring/summer period, of comparable accuracy as using the more time consuming traditional algorithm of Hammer (2000).

1 Introduction

For more than 20 years global irradiance at ground level has been successfully estimated from images taken by meteorological satellites. Since the input to the models is extremely simple, a single digital count per pixel, the methods need also to be very simple. So instead of a physical approach of using forward calculations and the principle of conservation of energy, the methods rely on the simple idea of using relative values of the digital counts:

- when a pixel is relatively dark, cloud free conditions are assumed, and the output of the model is simply global irradiance calculated with a clear sky model
- when the pixel is relatively bright, overcast conditions are assumed, and the output of the model is e.g. 5% of the corresponding clear sky value
- for intermediate brightness a simple linear transformation is assumed

On top of this scheme empirical corrections have been made with success, e.g. a subtraction of the scattered radiance from air molecules, which depends strongly on the geometry. Although such corrections improve the performance, they have some disadvantages:

- it is less obvious how to interpret physically the "relative reflectivity" and the cloud index

- corrections based on tuning to data may have unpredictable effects outside the specific sites or time periods which they are tuned to
- will new corrections describe a real physical phenomenon or just a side effect of earlier corrections?

Therefore, the number of corrections should be kept to a necessary minimum, and based on physical reasoning whenever possible. Here an analytical expression for the backscattered radiation from the atmosphere is derived and applied to the Heliosat-scheme. This removes the uncertainty related to the empirical expression from Hammer (2000) which could include components from aerosols and the sea surface, and which was also tuned to measurements for certain pixels for a certain time period. The analytical expression is also more straightforward to adapt to other sensors.

Another necessary procedure in the Heliosat-scheme is to compensate for the lower bound of the relative reflectivity (ρ_{ground}) which varies with time. The current approach in the Heliosat-scheme uses a histogram technique to determine the ground reflectivity for each slot (images acquired at the same UTC-time of day belong to the same "slot") and month, thus keeping the sun-ground-satellite geometry fairly constant. Some problems with this approach are:

- The number of data points available to find ρ_{ground} is maximum 31, which sometimes gives numerical unstabilities
- This procedure is a very time-consuming part of the Heliosat scheme

Besides, even for the same time of day, the geometry can change somewhat during a month. For Paris, as an example, the angle between the directions towards the sun and Meteosat for the 12 UTC slot is varying between 4 and 16 degrees during September. To overcome these problems, ρ_{ground} is parameterised as a function of the angle between the directions to the sun and satellite as seen from ground ("co-scattering angle"). In addition to saving computing time, this permits the use of a much lager data sample to determine ρ_{ground} , thus eliminating the problems for pixels and slots with few clear situations during a month.

2 An alternative algorithm for the cloud index

2.1 Calculation of the reflectivity from Meteosat counts

A part of the signal that a "visible" satellite sensor receives when viewing earth is directly scattered from air molecules. This part depends strongly on the sun-ground-satellite geometry, and as the radiation at ground is independent of the satellite position, it should be corrected for. The traditional approach in the Heliosat algorithm is to subtract a quantity from an expression which is tuned to satellite counts from cloud free pixels over sea (Hammer, 2000). It was however shown by Dagestad (2001) that most of this signal is first order scattered radiance, and hence an analytical expression for this component could be used. Under the assumption of a plane-parallel atmosphere the following expression for radiance scattered towards a satellite is derived (see Appendix):

$$r_{atm} = I_0 \frac{3(1+\cos^2\psi)}{16\pi} \frac{\cos\theta}{\cos\phi+\cos\theta}\left[1-e^{-\tau\left(\frac{1}{\cos\phi}+\frac{1}{\cos\theta}\right)}\right] \qquad (1)$$

where θ is the solar zenith angle, φ is the satellite zenith angle and ψ is the "co-scattering angle". $\boldsymbol{I_0}$ is the solar constant of 1367 W/m^2. According to the Appendix an optical depth $\boldsymbol{\tau}$ of 0.0426 is representative for the Meteosat-7 and 8 HRV channels, corresponding to an "equivalent wavelength" of 680 nanometres.

Equation 1 is singular for θ or φ at 90 degrees, but should have sufficient accuracy up to at least 85º

for a spherical atmosphere. The advantage of this expression compared to the one from Hammer (2000) is that it is not fitted to certain angular configurations, and that it contains no signal from the surface or other atmospheric components.

The reflectivity is then calculated by:

$$\rho = \frac{\pi (C - C_{off}) c_f}{\epsilon I_\mu \cos\theta} - \frac{\pi r_{atm}}{I_0 \cos\theta} \quad (2)$$

where:

- C is the raw Meteosat HRV counts
- C_{off} is the constant instrument offset (51 for Meteosat-8)
- $c_f = 0.56 \frac{W}{m^2 \cdot str \cdot \mu m \cdot counts}$ is the calibration constant and $I_\mu = 1403 \frac{W}{m^2 \cdot \mu m}$ is the band solar irradiance of the Meteosat-8 HRV channel (Govaerts et al., 2004)
- ε is the correction for varying sun-earth distance

The factor π is included to convert the reflected radiance to irradiance under the assumption of lambertian reflectance. This assumption is discussed in the next section. For the calculation of the cloud index ρ could be interpreted as the reflectivity of the ground and clouds, although this is not strictly physical correct.

2.2 Calculation of the cloud index from the reflectivity

In the Satel-Light version of the Heliosat scheme (Fontoynont et al., 1998) the (pseudo) ground reflectivity is determined for each pixel and for each month and slot. It is however seen that the reflectivity depends strongly on the co-scattering angle ψ, and thus a parameterisation will be made to correct for this. The correction probably includes the effects of:

- non-lambertian reflection from the ground surface itself
- varying amounts of shadows due to nearby terrain and broken clouds
- scattering and absorption due to interaction with air molecules, aerosols and clouds

Figure 1 shows the reflectivity according to Equation 2 plotted versus ψ for six sites in Europe and the Canary Islands. For each of these sites the 4-percentile value is calculated for ψ within each ten degree bin. A 3rd order polynomial is then fitted to these points, and plotted as broken curves on the figure. The mean of the polynomials is taken, and normalised to the value 1 for ψ = 0˚, to be used as a "shape function":

$$\rho_{g\,shape}(\psi) = 1 - 0.59\psi + 0.11\psi^2 + 0.05\psi^3 \quad (3)$$

where ψ is given in radians. The ground reflectivity can then be estimated by:

$$\rho_{ground}(\psi) = \rho_{g0}\,\rho_{g\,shape}(\psi) \quad (4)$$

where ρ_{g0} is the reflectivity of the pixel for ψ=0. This constant is determined by taking the 4-percentile of a time series of reflectivities divided by the "shape function". To avoid noise ψ should be kept below 50˚. The advantage of this approach is that the ground reflectivity can be determined once and for all, saving a lot of computer power. Besides, the difficulty of determining the reflectivity for months/slots with few clear situations is also avoided. ρ_{ground} from Equation 4 is plotted as solid lines on Figure1. Still the ground albedo can be determined more frequently to account for effects which are truly due to changes of the reflecting properties of the ground surface (e.g. snow cover and vegetative changes).

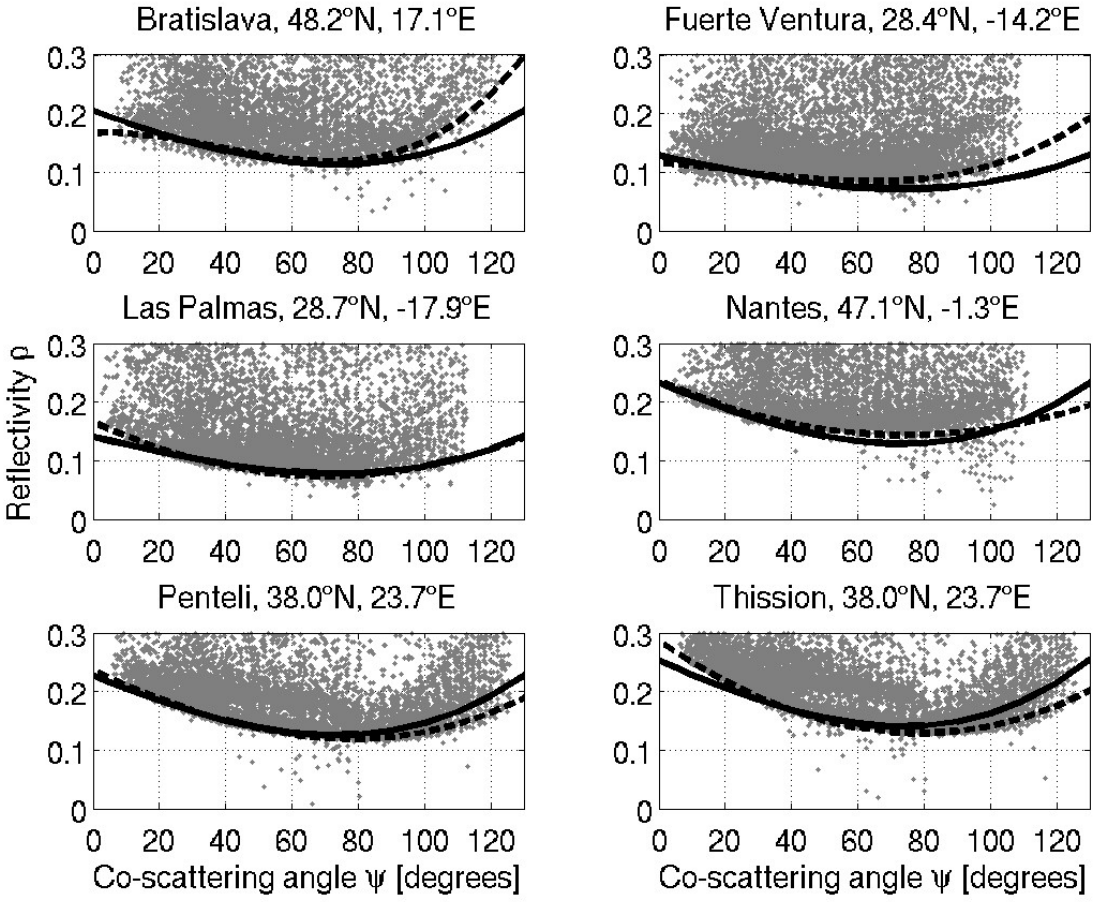

Figure 1: Reflectivities for the Meteosat-8 pixels of 6 European sites (dots) calculated with Equation 2 for all Meteosat-8 images between 16 March and 31 August 2004, plotted as a function of the co-scattering angle ψ. Broken lines: third order polynomials of ψ fitted to 4 percentiles within each ten degree bin (0-10, 10-20, etc). Solid lines: ground albedo calculated by Equation 4 by use of the procedure described in section 2.2

The upper boundary of reflectivities (cloud reflectivity) is seen to vary much less with ψ (or solar zenith angle θ) and a constant value of 0.81 is chosen as ρ_{cloud}, taken as the 98 percentile of the counts. This is assumed to be the reflectivity of the "thickest clouds". The 98 percentile is chosen instead of the maximum value to avoid any outliers. The cloud index (n) is then finally calculated from:

$$n = \frac{\rho - \rho_{ground}}{\rho_{cloud} - \rho_{ground}} \tag{5}$$

3 Description of data for validation

3.1 Ground measured global irradiances

In this study the satellite derived irradiances are compared to hourly measurements of global irradiances at five European stations for the period 16 March to 31 August 2004 (Table 1). All measurements are done with Kipp & Zonen pyranometers, and the data are manually quality controlled by the respective data providers (see acknowledgements).

Table 1: Stations with ground based hourly global irradiances.

Station	***Elevation [m.a.s.l.]***	***Latitude [°N]***	***Longitude [°E]***	***Instrument***
Barcelona	98	41.39	2.12	Kipp & Zonen CM 11
Bergen	45	60.40	5.32	Kipp & Zonen CM 11
Freiburg	275	48.02	7.84	Kipp & Zonen CM 11
Geneva	425	46.20	6.13	Kipp & Zonen CM 10
Lyon	170	45.78	4.93	Kipp & Zonen CM 6

3.2 Satellite derived global irradiances

Global irradiances are calculated by the following empirical relationship (Rigollier et al., 1998) using the cloud indices of section 2.1 as input:

$$k = \begin{cases} 1.2 & for\ n < -0.2 \\ 1-n & for\ n \in [-0.2, 0.8] \\ 2.0667 - 3.6667\, n + 1.6667\, n^2 & for\ n \in [\ 0.8, 1.1] \\ 0.05 & for\ n > 1.1 \end{cases} \tag{6}$$

The clear sky index k is defined as the ratio between the actual global irradiance, $\boldsymbol{G}$, and the clear sky global irradiance, $\boldsymbol{G_{clear}}$, which can be modelled with a clear sky model.

$$k \equiv \frac{G}{G_{clear}} \tag{7}$$

Two different clear sky models are used in this study:

- The model used by the Satel-Light project (Fontoynont et al., 1998) which consists of one model for the direct irradiance (Page, 1996) and one model for the diffuse irradiance (Dumortier, 1995). The input used is height above sea level, solar elevation and monthly values of Linke turbidities from a database developed by Dumortier (1998).

- The SOLIS model (Mueller et al., 2004) which uses two simulations with the radiative transfer model libRadtran (www.libRadtran.org) per day to parameterize the diurnal variation of global irradiance (and other spectral and angular components). SOLIS uses climatological values of water vapour (NVAP, www.stcnet.com/projects/nvap.html) and aerosols (SYNAER, Holzer-Popp et al., 2002a, 2002b) as input. Operational retrieval of aerosols and water vapour for input to SOLIS is planned for the near future within the EU-project Heliosat-3.

Two different cloud indices are also used:

- the cloud index calculated with the algorithm in section 2

- the "old" cloud index described in Hammer (2000). Adaptation from Meteosat-7 to Meteosat-8 was performed by Annette Hammer and Rolf Kuhlemann at the University of Oldenburg (personal communication) including a change of $\boldsymbol{\rho_{cloud}}$ from 160 counts to 650 counts (Meteosat-8 gives 10-bit values, whereas Meteosat-7 gives 8-bit values)

4 Validation

4.1 Verification of the algorithm for calculation of ground reflectivity

In section 2.2 a new method to calculate the ground reflectivity in Heliosat was developed. This method will here be validated against five stations which are independent from the stations used for development. Figure 2 shows reflectivities calculated with Equation 2 from the hourly means of the satellite counts for the five stations in table 1. It is seen that the ground albedo calculated with the algorithm of section 2.2 is nicely fitting the lower bound of reflectivities. The fit is actually better than for the development stations; the reason for this is that the averaging of four 15 minute values to create hourly values is removing much of the "noise" seen in the plot of 15-minute values on Figure 1. The shape function (Equation 3) describes well the non-lambertian variation of reflectivity for all stations, even though ρ_{g0} varies between 0.165 for Bergen and 0.208 for Barcelona and Lyon.

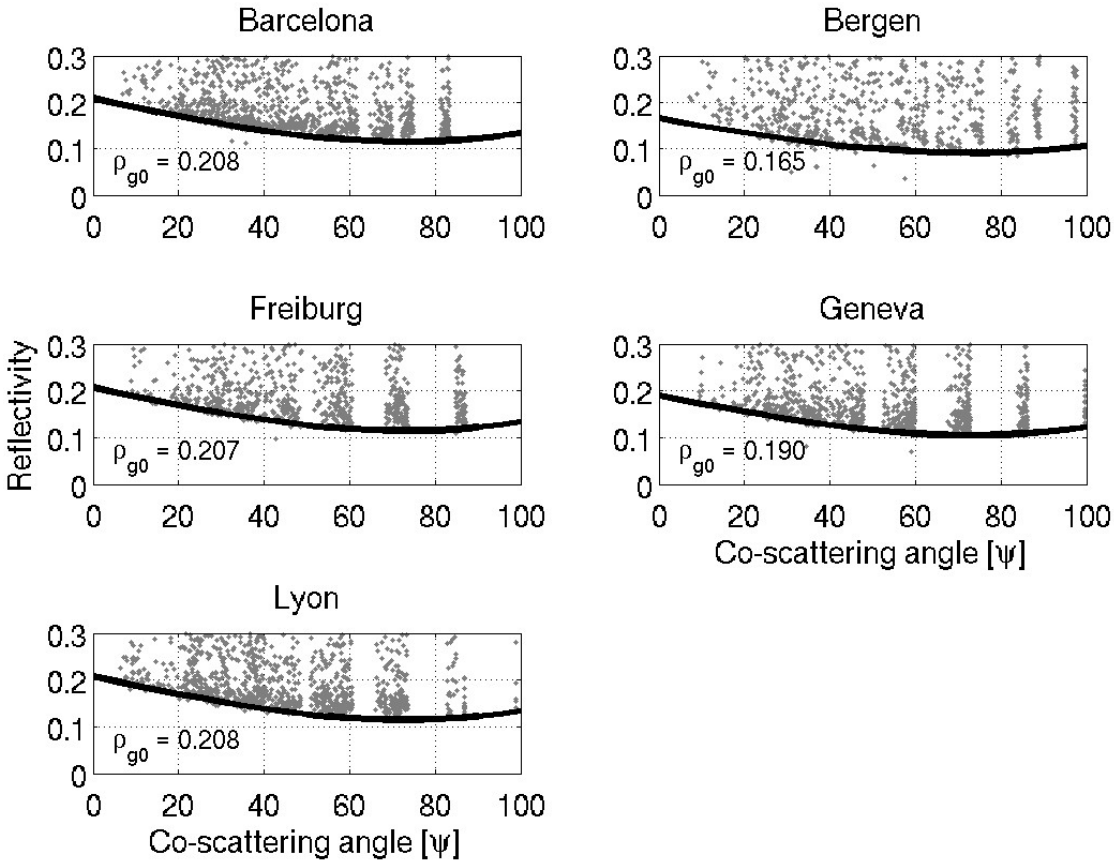

Figure 2: Calculated reflectivities for the hourly means of the satellite counts for the stations of Table 1 (points). Ground albedo from the algorithm in section 2.1 is plotted as solid lines.

4.2 Optimal pixel size

In earlier versions of Heliosat, with data from Meteosat First Generation (MFG, Meteosat 1-7), the best accuracy was obtained by averaging cloud indices over 15 pixels, 5 pixels in the east -west direction and 3 pixels in the north-south direction (Fontoynont et al., 1998). To find the optimal pixel size for Meteosat-8, cloud indices are here calculated for the following configurations: single pixel, 3x3, 5x5, 7x7 and 1x3, 3x5, 5x7 and 7x9. The n times (n+2) configurations gives an approximately square area in Europe where pixels are longer in the north-south direction due to

oblique viewing angle. Figure 3 shows the Root Mean Square Deviation (RMSD) of hourly global irradiances for all five ground stations. Only results with the Satel-Light clear sky model are shown, but both the old and the new cloud indices are used. For both cloud indices and for all stations, averaging over 3x5 pixels gives the lowest RMSD. (The only exception is Lyon where 5x5 pixels gives slightly lower RMSD). This is the same results as for MFG, even though the MSG pixels have roughly nine times smaller area. In this study all irradiances are hereafter calculated with cloud indices averaged over 3x5 pixels.

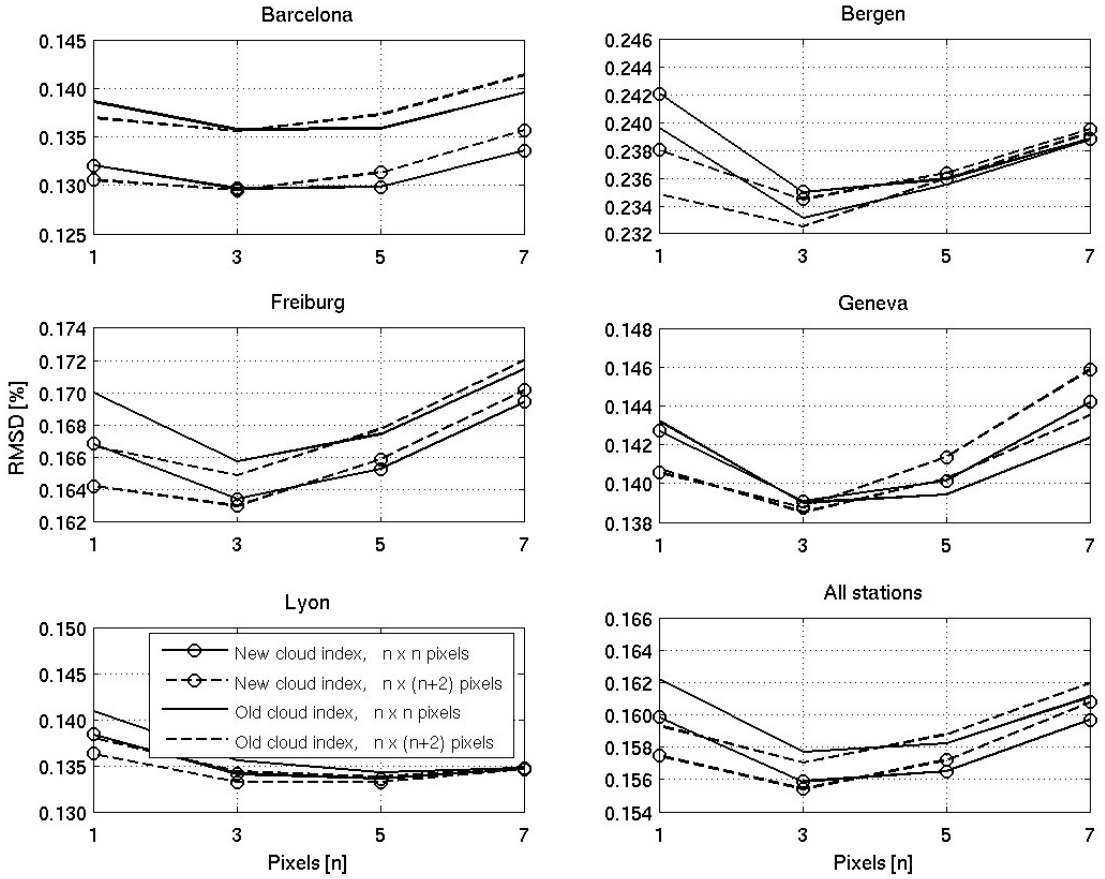

Figure 3: Root Mean Square Deviation (RMSD) of hourly global irradiances calculated with the Heliosat-method, using two different cloud indices. For the solid lines the cloud indices are averages over n x n pixels; for the broken lines the number of pixels in the east-west direction is n+2.

4.3 Validation of hourly global irradiances

Table 2 shows RMSD and Mean Bias Deviation (MBD, model-observation) for all stations and for both cloud indices and both clear sky models (chapter 3). Only hours for which the solar elevation is always above 5 degrees are compared. For the average over all stations the new cloud index with the Satel-Light clear sky model gives the lowest RMSD (15.5%) and also the smallest MBD (-0.9%). However, when the SOLIS clear sky model is used the old cloud index performs better, and the global irradiances calculated with the new index are then on average 3% too low.

Table 2: Root Mean Square Deviation (RMSD) and Mean Bias Deviation (MBD, model-observation) for two different clear sky models (SOLIS, Satel-Light) and two different cloud indices ("New" and "Old", see chapter 3). The values are given in percent of mean observed global irradiance. Bold numbers show the lowest RMSD for the given station.

			New cloud index				***Old cloud index***			
			SOLIS		Satel-Light		SOLIS		Satel-Light	
Station	Observed [W/m^2]	Number of hours	RMSD	MBD	RMSD	MBD	RMSD	MBD	RMSD	MBD
Barcelona	531	1475	14.7	-6.4	**12.9**	1.1	13.7	-3.9	13.6	3.8
Bergen	280	2073	23.4	0.2	23.5	0.4	**23.1**	0.0	23.3	0.2
Freiburg	389	1753	17.1	-6.0	**16.3**	-2.2	16.5	-3.3	16.5	0.6
Geneva	459	1656	14.0	-3.1	13.9	-2.3	**13.8**	-0.6	13.9	0.2
Lyon	432	2003	**13.1**	0.4	13.3	-1.3	13.6	2.5	13.4	0.8
All stations	410	8960	16.1	-3.0	**15.5**	-0.9	15.7	-1.0	15.7	1.2

Table 2 gives no unique answer to which is the best cloud index and which is the best clear sky model. According to Table 3 the Satel-Light clear sky model generally gives higher clear sky irradiances than the SOLIS model, and Figure 4 shows that the new cloud index is generally higher than the old one. Hence a too high cloud index can compensate for a too high clear sky value and vice versa. The frequency distributions of Figure 4 show that the new cloud index has a clear peak close to zero, while the old one has more frequently negative values. Negative cloud indices give clear sky indices higher than 1, which could compensate for a clear sky model giving too low values. For the clear sky models it should be stressed that the input to the models is probably more important than the models themselves, so an interesting prospect for the near future is the inclusion of daily retrieved atmospheric parameters into the SOLIS model within the Heliosat-3 project. The new cloud index has however the advantage of being fast and easy to calculate routinely, and as it is based on physical quantities it should be easier to do possible physical and/or empirical corrections in the future.

Table 3: Mean clear sky global irradiances of all hours for all stations and both clear sky models. See chapter 3 for description of the models.

	SOLIS	Satel-Light
Barcelona	613.1	662.2
Bergen	484.2	484.6
Freiburg	576.9	600.5
Geneva	605.9	610.8
Lyon	606.2	595.5
All stations	573.3	584.6

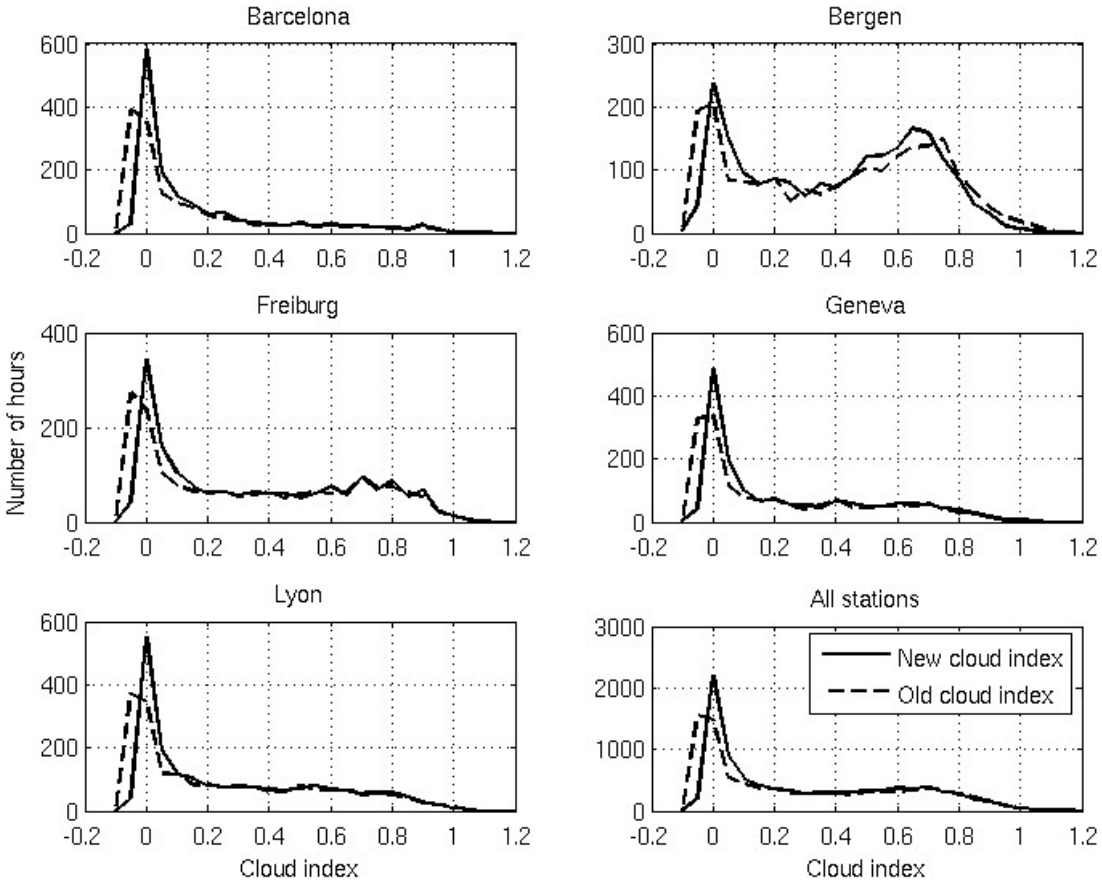

Figure 4: Frequency distributions of the two different cloud indices for the five stations of Table 1.

5 Summary and discussion

Two modifications are made to the traditional algorithm for calculation of the cloud index:

- An analytical expression for the scattered radiance from air molecules is introduced, replacing an empirical expression.
- The variation of the parameter ρ_{ground} is parameterised as a function of the angle between the directions towards the sun and the satellite. This permits to calculate ρ_{ground} once and for all, replacing a time consuming histogram technique which has to be applied separately to each slot and month.

These two corrections are applied in the Heliosat scheme to calculate global irradiances and the results are compared to hourly measurements from five ground stations in Europe. The RMSD and the MBD are very similar compared to the results using the traditional cloud index from Hammer (2000). One cloud index gives however better results with one clear sky model, while the other cloud index gives better results with another clear sky model. It is seen that the Satel-Light clear sky model generally gives higher values than SOLIS, and that the new cloud index introduced here is generally higher than the one from Hammer (2000). Thus it is evident that sometimes errors are cancelling each other in the Heliosat-scheme, and sometimes they are adding up. Using climatological values of turbidity as input to the clear sky models, the clear sky model is by now a large uncertainty in the Heliosat-scheme. This makes it difficult to find the optimal cloud index. The inclusion of real time atmospheric parameters in the new SOLIS clear sky model in the near future looks promising. As the clear sky value will then have a stronger physical basis, both the cloud index and the relationship with the clear sky index should be suitably chosen, and perhaps

tuned to ground data to minimise the deviation. The remaining empirical parameters which can be adjusted for best performance are:

- The method to determine ρ_{cloud}. Here a 98 percentile of reflectivities is used, but there is no clear physical reasoning behind such a choice. The bias of the Heliosat-algorithm is highly sensitive to the choice of $\rho_{cloud.}$
- The method to determine $\rho_{ground.}$ The bias is not as sensitive to this parameter, as it is in both the nominator and denominator of equation 5, but it should certainly be chosen so that when the reflectivity equals ρ_{ground}, the observed clear sky value is matching the clear sky model.
- The clear sky - cloud index relationship. For the cloud index approaching 1 the value of the clear sky index should be in accordance with the value of $\rho_{cloud.}$ In other words; the clear sky value for the cloud index equal to 1 should be similar to what is observed under a cloud cover giving a reflectivity equal to $\rho_{cloud.}$

It is seen that the new cloud index has a clear peak around zero, while the traditional has more frequently negative values. The reason is that the old histogram technique gives a higher value for ρ_{ground} than the new algorithm presented in section 2.2. There are two ways the cloud index can become negative; one is when the atmosphere is clearer than the "reference atmosphere" for which the clear sky model applies. For this case a negative cloud index gives correctly a global irradiance which is higher than the clear sky model. A second reason can be that the pixel is completely in shadow from a nearby cloud which is not seen on this pixel. In this case the conditions are taken as very clear, while the ground measured irradiance is low due to the shadows. Probably both situations occur, and the effects are cancelling each other. That the 'traditional' cloud index is more frequently negative needs not be a bad sign, but one should be aware of the difference when it is combined with a clear sky model.

For both cloud indices and clear sky models averaging the cloud index over 3x5 pixels gives best results.

Acknowledgements:
This work is a part of the project Heliosat-3 funded by the European Commission (NNK5-CT-200-00322). We thank project colleagues for valuable discussions and advices. The following persons are thanked for providing the ground measurements for the validation: Antonio Ortegón Gallego (Barcelona), Christian Reise (Freiburg), Pierre Ineichen (Geneva) and Dominique Dumortier (Lyon). We also thank Jethro Betcke and Rolf Kuhleman at the University of Oldenburg for providing data from Meteosat-8 for specific sites.

6 References

Rigollier, C; Lefèvre, M; Wald, L (2004) The method Heliosat-2 for deriving shortwave solar radiation from satellite images, Solar Energy 77, 159-169
Hammer, A (2000) Anwendungsspezifische Solarstrahlungsinformationen aus Meteosat-daten, PhD thesis, University of Oldenburg
Dagestad, K-F (2001) Ein modellstudie av samanhengen mellom reflektert radians ved toppen av atmosfæra og globalstråling ved bakken, Master Thesis, University of Bergen
Govaerts, Y; Clerici, M (2004) MSG-1/SEVIRI Solar Channel Calibration, ; Commisioning Activity Report for Eumetsat. EUM/MSG/TEN/04/0024, Version 1.0, 21 Jan 2004
Fontoynont, M; Dumortier, D; Heinemann, D; Hammer, A; Olseth, J A; Skartveit; Ineichen, P; Reise, C; Page, J; Roche, J; Beyer, H; Wald, L (1998) Satel-Light: A www server which provides high quality daylight and solar radiation data for western and central Europe, Proc. 9th conference on satellite meteorology and oceanography in Paris, 25-28 May 1998, pp. 434-437

Rigollier, C.; Wald, L. (1998) Using Meteosat images to map the solar radiation:improvements of the Heliosat method, Proceedings of the 9th Conference on Satellite Meteorology and Oceanography. Published by Eumetsat, Darmstadt,Germany, EUM P 22, pp. 432-433
Page, J (1996) Algorithms for the Satel-Light programme, Technical report for the Satel-Light programme
Dumortier, D (1995) Modelling global and diffuse horizontal irradiances under cloudless skies with different turbidities, Technical report for the Daylight II project, JOU2-CT92-0144
Dumortier, D (1998) The Satel-Light model of turbidity variations in Europe, Report for the 6th Satel-Light meeting in Freiburg, Germany, September 1998
Mueller, R; Dagestad, K-F; Ineichen, P; Schroedter, M; Cros, S; Dumortier, D; Kuhlemann, R; Olseth, J. A; Piernavieja, C; Reise, C; Wald, L; and Heinemann, D (2004) Rethinking satellite-based solar irradiance modelling, The SOLIS clear sky module, Remote Sensing of the Environment 91, 160-174
Holzer-Popp, T; Schrodter, M; Gesell, G (2002a) Retrieving aerosol optical depth and type in the boundary layer over land and ocean from simultaneous GOME spectrometer and ATSR-2 radiometer measurements, 1, Method description, J. Geophys. Res. 107, AAC16-1 – AAC16-17
Holzer-Popp, T; Schrodter, M; Gesell, G (2002b) Retrieving aerosol optical depth and type in the boundary layer over land and ocean from simultaneous GOME spectrometer and ATSR-2 radiometer measurements, 2, Case study application and validation, J. Geophys. Res.
Paltridge, G; Platt, C (1976) Radiative processes in meteorology and climatology, Elsevier, ISBN 0-444-41444-4

Appendix

A.1 An analytical expression for the backscattered radiation from air molecules

An analytical expression for the scattered radiance from the air molecules towards a satellite will here be derived for plane-parallel conditions. It is assumed that there are no other scattering or absorbing agents in the atmosphere, and that all photons are scattered only once. Figure 5 shows a situation with a solar zenith angle $\boldsymbol{\theta}$, and a satellite viewing the sunlit area at ground with a zenith angle $\boldsymbol{\varphi}$. The optical depth due to scattering is increasing downwards from 0 at the top of atmosphere to $\boldsymbol{\tau}$ and $\boldsymbol{\tau+d\tau}$ at two indicated levels.

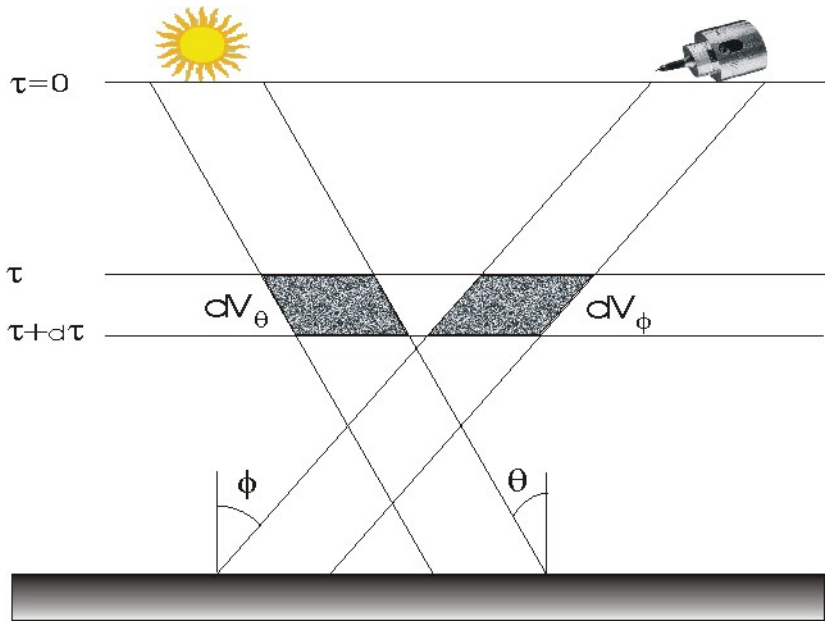

Figure 5: Schematic illustration of the infinitesimal volumes of the atmosphere between the optical depth τ and τ + δτ from which solar radiation is scattered towards a satellite. θ and φ are the solar and satellite zenith angles, respectively.

The amount of radiation scattered per volume unit at level $\boldsymbol{\tau}$ is given by:

$$\frac{direct\ \ radiation\ into\ \ volume\ \ dV_\theta - direct\ \ radiation\ out\ \ of\ \ dV_\theta}{dV_\theta} = \frac{I_\lambda e^{\frac{-\tau}{\cos\theta}} - I_\lambda e^{\frac{-\tau+d\tau}{\cos\theta}}}{\frac{d\tau}{\cos\theta}} = \frac{\cos\theta}{d\tau} I_\lambda e^{\frac{-\tau}{\cos\theta}} (1 - e^{\frac{-d\tau}{\cos\theta}}) \approx I_\lambda e^{\frac{-\tau}{\cos\theta}} \tag{8}$$

where $\boldsymbol{I_\lambda}$ is the incoming monochromatic irradiance at the top of the atmosphere.

The scattered radiation from the volume $\boldsymbol{dV_\varphi}$ that reaches the satellite is given by:

$$\frac{scattered\ radiation}{unit\ volume} \times phase\ function \times transmissivity\ towards\ satellite \times volume = I_\lambda e^{\frac{-\tau}{\cos\theta}} P(\psi) e^{\frac{-\tau}{\cos\phi}} \frac{d\tau}{\cos\phi} \tag{9}$$

where $\boldsymbol{P(\psi)}$ is the scattering phase function and $\boldsymbol{\psi}$ is the angle between the directions towards the sun and satellite as seen from ground. Integration from $\boldsymbol{\tau} = 0$ at the top of the atmosphere to $\boldsymbol{\tau}$ gives the scattered radiance towards the satellite from the whole atmospheric column down to the level $\boldsymbol{\tau}$:

$$r_\lambda = \frac{I_\lambda P(\psi)}{\cos\phi} \int_0^\tau e^{-\tau'(\frac{1}{\cos\theta}+\frac{1}{\cos\phi})} d\tau' = I_\lambda P(\psi) \frac{\cos\theta}{\cos\phi + \cos\theta} [1 - e^{-\tau(\frac{1}{\cos\theta}+\frac{1}{\cos\phi})}] \tag{10}$$

The Rayleigh scattering function is well known:

$$P(\psi)=\frac{3}{16\pi}(1+\cos^2\psi) \tag{11}$$

Note that in this context ψ is 180 degrees minus the more commonly used scattering angle, and is therefore referred to as the 'co-scattering angle'. Equation 11, however, remains unchanged. An expression for the vertical optical depth of the atmosphere due to Rayleigh scattering as a function of wavelength is found from Paltridge et al. (1976):

$$\tau=\left(\frac{\lambda}{0.311\,\mu m}\right)^{-4.05} \tag{12}$$

A.2 Adaptation to the Meteosat-8 HRV response function

Equations 10, 11 and 12 describe monochromatic radiation scattered towards a satellite. To get the actual radiance observed by Meteosat it should be integrated over all wavelengths, weighted with the Meteosat-8 HRV response function:

$$r_{atm}=\frac{\int r_\lambda R_{HRV}\,d\lambda}{\int R_{HRV}\,d\lambda} \tag{13}$$

Then the equation would have to be integrated numerically for any actual geometrical configuration. Figure 6 shows that by using an 'equivalent wavelength' of 680 nanometres radiances very close to what is obtained by numerical integration over all wavelengths are found. To a good approximation the following equation can therefore be used for the scattered solar radiation from air molecules reaching Meteosat-8:

$$r_{atm}=I_0\frac{3(1+\cos^2\psi)}{16\pi}\frac{\cos\theta}{\cos\phi+\cos\theta}\left[1-e^{-\tau\left(\frac{1}{\cos\phi}+\frac{1}{\cos\theta}\right)}\right] \tag{14}$$

where I_0 is the solar constant of 1367 W/m^2. Equation 12 gives a value for the optical depth τ of 0.0426 for λ = 680 nanometres.

The same equation can be used for Meteosat-7 which has the same spectral response function of the HRV-channel. For other spectral channels similar 'equivalent wavelengths' could be obtained by the same integration. It was shown in Dagestad (2001) that for the wavelengths of the Meteosat HRV function single scattering is dominant. Care should however be taken for wavelengths where multiple scattering is dominant.

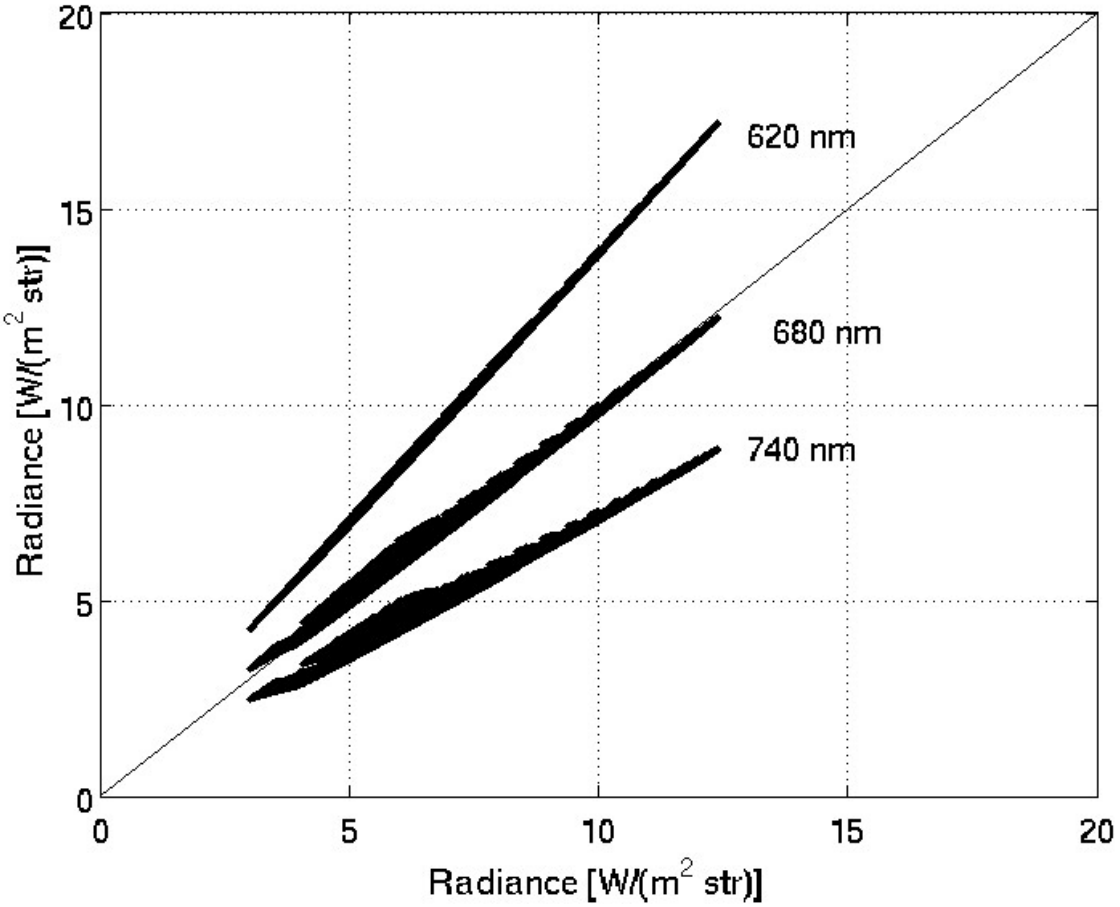

Figure 6: Calculation of the radiance scattered from air molecules and observed by the Meteosat-8 HRV channel for various angular configurations. The x-axis is the result obtained by numerically integrating Equation 13. The y-axis is the results by using Equation 14 with optical depths for the wavelengths indicated on the figure. The geometrical configurations used are the actual configurations for all Meteosat-8 images for the period 16 March to 31 August 2004 for the same stations as in Figure 1.